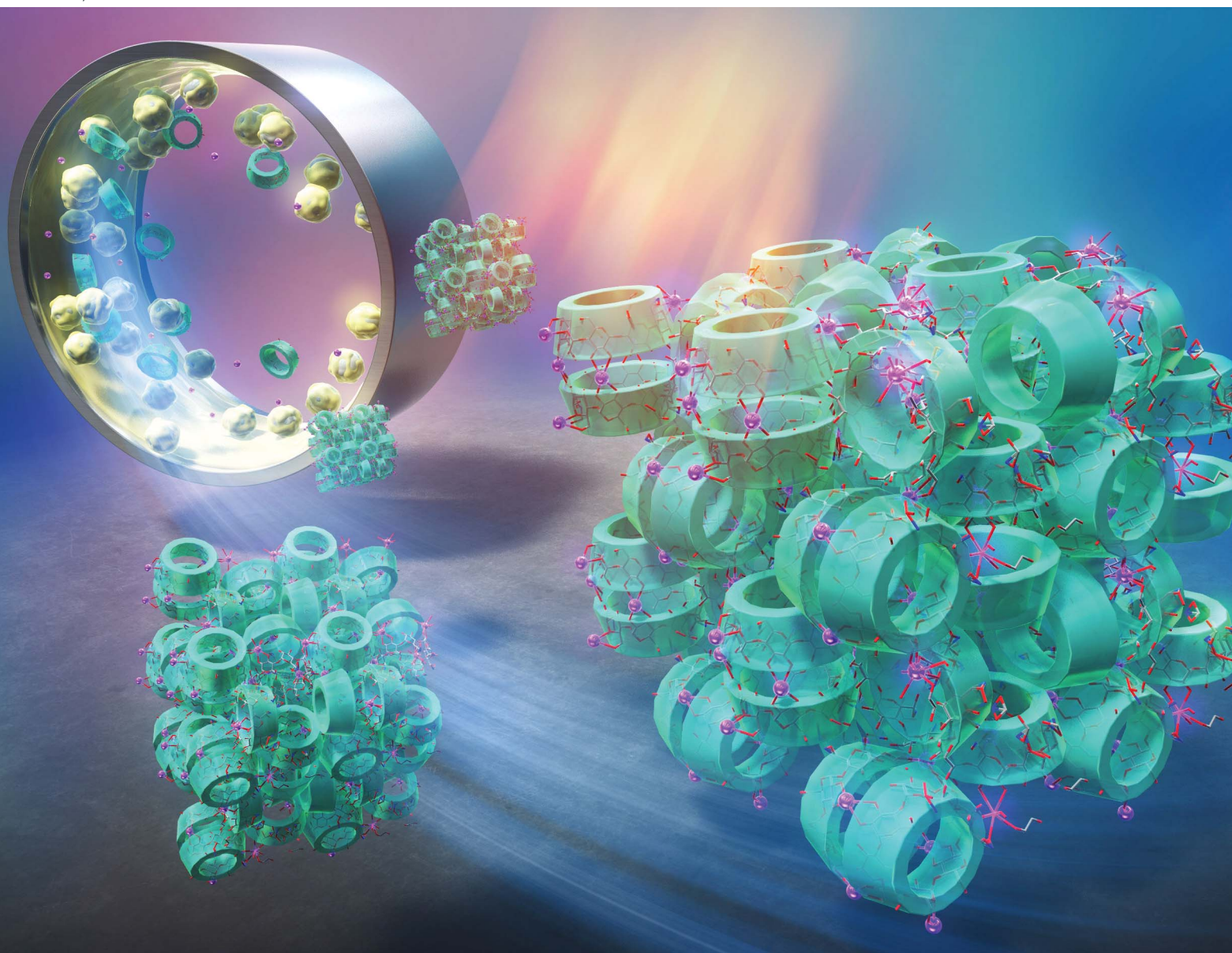


# RSC Mechanochemistry

[rsc.li/RSCMechanochem](https://rsc.li/RSCMechanochem)



ISSN 2976-8683

Cite this: *RSC Mechanochem.*, 2024, 1, 153Received 21st October 2023  
Accepted 9th February 2024

DOI: 10.1039/d3mr00006k

rsc.li/RSCMechanochem

## “Wash-free” synthesis of cyclodextrin metal–organic frameworks†

Shuhei Fujita,<sup>a</sup> Kazunori Kadota,<sup>b</sup> Atsushi Koike,<sup>c</sup> Hiromasa Uchiyama,<sup>b</sup> Yuichi Tozuka<sup>b</sup> and Shunsuke Tanaka<sup>b</sup>   <sup>ad</sup>

Herein, we propose a simple and fast synthetic strategy for preparing highly crystalline  $\gamma$ -cyclodextrin-based metal–organic frameworks (solid yield 100%). This is the first method that allows metal–organic frameworks with high surface areas to be synthesised without a washing step.

While there is a great deal of scientific research on stable metal–organic frameworks (MOFs) for gas storage, separation and catalysis,<sup>1,2</sup> the development and application of MOFs in health and medicine remains a major challenge. In general, biocompatible linkers can be selected as part of the MOF structure, of which the cyclic oligosaccharide cyclodextrins (CDs) are a shrewd choice.<sup>3,4</sup> Although CD-based MOF materials are still in the early stages of research and development and there are many obstacles to overcome in their design and manufacture, the advantages derived from CD assembling porous frameworks are exciting. CDs are classified according to the number of glucopyranose units in the molecule as  $\alpha$ -CD (hexamer),  $\beta$ -CD (octamer) and  $\gamma$ -CD (octamer).<sup>5,6</sup> Among them,  $\gamma$ -CD and alkali metal salts are complexed and crystallized to form the nanoporous CD-MOF crystals.<sup>7,8</sup> The interior of the macrocyclic ring of  $\gamma$ -CD, in which glucose subunits are joined by  $\alpha$ -1,4-glycosidic bonds, is hydrophobic, while its exterior is hydrophilic. Within the CD-MOF crystals, pairs of  $\gamma$ -CD combine to form

a barrel-like structure, the interior of which is a hydrophobic nanopore. On the other hand, when the ( $\gamma$ -CD)<sub>6</sub> unit crystallizes, a spherical hydrophilic nanopore is formed at its center. The hydrophobic and hydrophilic pores are connected like a necklace of pearls, and once molecules larger than about 0.8 nm in diameter, corresponding to the narrowest opening, are encapsulated in the pore, they are expected not to be released unless the crystal structure collapses.

The pursuit of commercial availability of MOFs is essential to advance the social implementation of MOFs in biochemical, pharmaceutical and food engineering. Among the most important challenges are the limited availability and high cost of commercially available MOFs and, above all, the difficulty of scaling up synthesis in a cost-effective manner while maintaining product quality. The cost of MOFs depends on the raw material costs (ligands, metal sources and solvents) and the manufacturing process (product recovery by filtration and other means, washing, drying, forming and processing), including capital investment, process energy, utilities and labor costs.<sup>9,10</sup> To address process simplification and cost reduction, various synthesis methods have been demonstrated, including solvothermal, hydrothermal, microwave-assisted,<sup>11,12</sup> sonochemical,<sup>13,14</sup> microfluidic,<sup>15,16</sup> aqueous solution,<sup>17,18</sup> spray-drying<sup>19–22</sup> and mechanochemical methods.<sup>23–27</sup> To date, the most conventional and common method for obtaining CD-MOF crystals is the vapor diffusion method.<sup>7,8</sup> In the vapor diffusion method, an aqueous solution of a metal salt and  $\gamma$ -CD in an appropriate ratio is placed in a glass container and left for several days under methanol diffusion. CD-MOFs consisting of K<sup>+</sup>, Rb<sup>+</sup> and Cs<sup>+</sup> have been successfully synthesized by methanol diffusion into an aqueous solution containing one equivalent of  $\gamma$ -CD and eight equivalents of each metal salt for a week.<sup>28,29</sup> Although the vapor diffusion method is reliable and reproducible, it is time-consuming and requires solubility of the ligand, which limits its practical application for MOF production. Aqueous solution and mechanochemical methods have the potential advantages of mass production, high yields and avoidance of large amounts of organic solvents and high

<sup>a</sup>Department of Chemical, Energy, and Environmental Engineering, Faculty of Environmental and Urban Engineering, Kansai University, Suita, Osaka 564-8680, Japan. E-mail: shun\_tnk@kansai-u.ac.jp; Web: <https://wps.its.kansai-u.ac.jp/sepsyseng/>

<sup>b</sup>Department of Formulation Design and Pharmaceutical Technology, Faculty of Pharmacy, Osaka Medical and Pharmaceutical University, Takatsuki, Osaka 569-1094, Japan

<sup>c</sup>Department of Pathobiochemistry, Faculty of Pharmacy, Osaka Medical and Pharmaceutical University, Takatsuki, Osaka 569-1094, Japan

<sup>d</sup>Collaborate Research Center of Engineering, Medicine and Pharmacology (CEMP), Organization for Research and Development of Innovative Science and Technology (ORDIST), Kansai University, Suita-shi, Osaka 564-8680, Japan

† Electronic supplementary information (ESI) available. See DOI: <https://doi.org/10.1039/d3mr00006k>

temperatures. The mechanochemical method, a well-known technique in metallurgy and mineral processing, has expanded the scope of its application to MOF synthesis in the last decade, leading to exciting research and development.<sup>30,31</sup> The key idea behind this synthetic method is to accelerate the chemical reaction by exerting mechanical stresses to solid starting materials, minimizing or even eliminating the use of solvents. However, note that an activation step, in which the solid product is washed with an organic solvent, is necessarily essential for MOF synthesis. The mechanochemical method (as well as aqueous solution method) is no exception to this rule.<sup>32</sup>

Nevertheless, the mechanochemical method is the most environmentally friendly methodology and is therefore expected to be an economically promising MOF production process. In this study, a mechanochemical method for CD-MOF was developed for the first time, in which the product washing step was eliminated.

The synthesis procedure is very simple and can be reproduced by anyone.  $\gamma$ -CD and the potassium source ( $\text{KHCO}_3$ ,  $\text{CH}_3\text{COOK}$ ,  $\text{KOH}$ ,  $\text{KCl}$  or  $\text{K}_2\text{CO}_3$ ) together with a small amount of ethanol were placed in a 250 mL zirconia milling jar containing 30 YTZ® balls. Typically, the molar ratio of mixture is  $\gamma\text{-CD} : \text{K}^+ : \text{ethanol} = 1 : 2 : 0.04$ ; the  $\text{K}^+/\text{CD}$  ratio can be varied from 0.67 to 8 and the ethanol/CD ratio can be reduced to 0.0085. These were then milled at a rotation rate of 150 rpm for 5 min by using a planetary mill Pulverisette 6 (Fritsch Japan). The products were only dried under atmospheric pressure at 80 °C for 1 h. Since this method only involves milling and drying, the final product can be obtained in 100% solid yield.

Fig. 1 shows the PXRD patterns of the products prepared with mechanochemical treatment.  $\text{KHCO}_3$  was used as the  $\text{K}^+$  source in these syntheses. Surprisingly, the dried products of the mixture of CD,  $\text{KHCO}_3$  and ethanol showed diffraction peaks attributed to the (110), (200), (211) and (220) planes of the CD-MOF crystal at  $2\theta = 4.0, 5.6, 7.1$  and  $13.3^\circ$ , respectively.<sup>7</sup> The crystal structure of CD-MOF was confirmed by the Rietveld refinement. However, it was also found that some  $\text{KHCO}_3$

remained unreacted when the  $\text{K}^+/\text{CD}$  ratio was higher than 4. On the other hand, without mechanochemical treatment, some  $\text{KHCO}_3$  remained unreacted and further unidentified by-products were formed, as shown in Fig. S1 (ESI).† Mechanochemical treatment for only 5 min dramatically improved the yield of CD-MOF. The PXRD patterns of CD-MOFs prepared with other potassium sources ( $\text{CH}_3\text{COOK}$ ,  $\text{KOH}$ ,  $\text{KCl}$  and  $\text{K}_2\text{CO}_3$ ) are shown in Fig. S2 (ESI).†

Our synthetic method allows the production of CD-MOF without the need for a washing step. As the washing step is not required, the addition of excess potassium sources, which are not necessary for the structural formation of CD-MOF, increases the amount of unreacted potassium. The stoichiometric ratio of the coordination reaction between  $\text{K}^+$  and  $\gamma\text{-CD}$  is  $\text{K}^+/\text{CD} = 2$ . In conventional synthetic methods such as vapor diffusion and poor solvent crystallization, it is common to add excess  $\text{K}^+$  to  $\gamma\text{-CD}$  and it is essential that the unreacted potassium is removed by washing. Excess  $\text{K}^+$  is not completely removed by washing and the composition of CD-MOF,  $\text{K}^+/\text{CD}$ , is usually larger than 2. In contrast, our method has resulted in the formation of a crystal structure of CD-MOF with  $\text{K}^+/\text{CD}$  less than 2.

The thermogravimetric curves of  $\text{KHCO}_3$ ,  $\gamma\text{-CD}$  and CD-MOF are shown in Fig. 2. It is well known that the thermal stability of CD-MOF is lower than that of the raw material  $\gamma\text{-CD}$ . This is because the presence of the potassium source promotes the pyrolysis of organic material  $\gamma\text{-CD}$ . This is the reason why the thermogravimetric loss of CD-MOFs with low  $\text{K}^+/\text{CD}$  ratios shifted towards higher temperatures. The weight loss of CD-MOFs increased with decreasing  $\text{K}^+/\text{CD}$  ratios because potassium-derived substances remain as residues after pyrolysis. The thermogravimetric curves of CD-MOFs prepared with other potassium sources ( $\text{CH}_3\text{COOK}$ ,  $\text{KOH}$  and  $\text{KCl}$ ) are shown in Fig. S3 (ESI).† The pyrolysis behaviour depends on the potassium source. Among them, CD-MOFs prepared with  $\text{KCl}$  have the highest thermal stability.

The nitrogen adsorption/desorption isotherms of unwashed CD-MOFs are shown in Fig. 3. Table 1 shows the BET area and total pore volume of CD-MOFs. The original  $\gamma\text{-CD}$  is non-porous as it does not adsorb nitrogen at 77 K. In contrast, the products obtained by the reaction of  $\gamma\text{-CD}$  with potassium sources ( $\text{KHCO}_3$ ,  $\text{CH}_3\text{COOK}$ ,  $\text{KOH}$ ,  $\text{KCl}$  or  $\text{K}_2\text{CO}_3$ ) in this study could

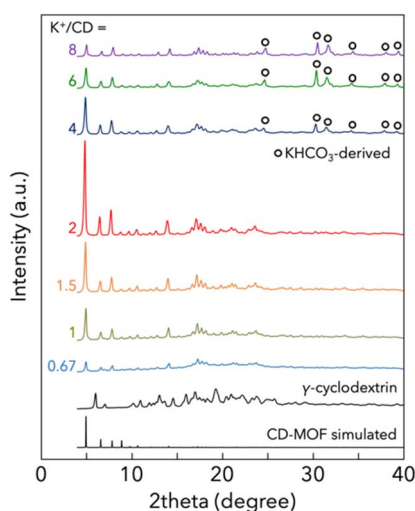


Fig. 1 PXRD patterns of the products prepared with mechanochemical treatment.

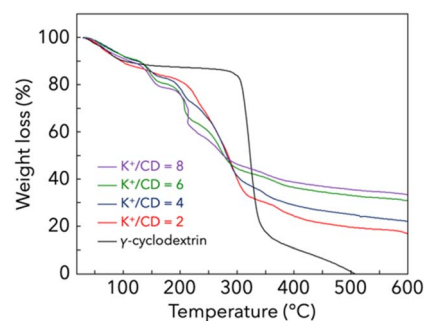


Fig. 2 Thermogravimetric curves of  $\gamma\text{-CD}$  and CD-MOFs. CD-MOFs were prepared by wash-free mechanochemical synthesis with different  $\text{K}^+/\text{CD}$  ratios using  $\text{KHCO}_3$ .





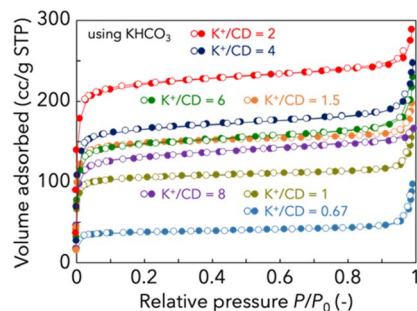


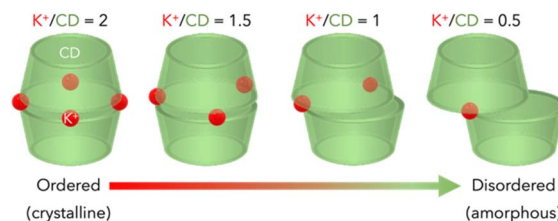
Fig. 3  $N_2$  adsorption/desorption isotherms of CD-MOFs prepared by wash-free mechanochemical synthesis. Before the measurements, the samples were degassed at 50 °C under vacuum for 6 h.

Table 1 Structural characteristics of CD-MOFs

Potassium source	$K^+/CD$	$S_{BET}^a/m^2 g^{-1}$	$V_{total}^b/cm^3 g^{-1}$
$KHCO_3$	8	527	0.253
$KHCO_3$	6	574	0.339
$KHCO_3$	4	655	0.362
$KHCO_3$	2	906	0.373
$KHCO_3$ (washed) <sup>c</sup>	2	368	0.173
$KHCO_3$	1.5	600	0.306
$KHCO_3$	1	415	0.238
$KHCO_3$	0.67	143	0.137
KCl	2	878	0.438
KOH	2	698	0.401
$CH_3COOK$	2	631	0.370
$K_2CO_3$	2	30.0	0.057
(Vapour diffusion method) <sup>d</sup>		803	0.322
(CD-MOF-1) <sup>e</sup>		1220	0.48
( $\gamma$ -CD) <sup>f</sup>		1	0.009

<sup>a</sup> BET area. <sup>b</sup> Total pore volume. <sup>c</sup> Product washed after mechanochemical treatment. <sup>d</sup> CD-MOF prepared at  $K^+/CD = 8$  by the vapour diffusion method according to the literature.<sup>7</sup> <sup>e</sup> CD-MOF-1 reported in the literature.<sup>7</sup> Note that the activation conditions before  $N_2$  adsorption measurements are different. <sup>f</sup> Original  $\gamma$ -CD.

adsorb nitrogen and have relatively high BET areas, as shown in Fig. S4 (ESI).<sup>†</sup> As the  $K^+/CD$  ratio increased from 0.67 to 2, the BET area of CD-MOF increased, reaching a maximum at  $K^+/CD = 2$ , and decreased as the  $K^+/CD$  was further increased. The lower BET area in the case of low potassium source addition is due to a low degree of crystallization. On the other hand, the low BET area in the case of excess potassium source addition is due to the presence of the unreacted potassium source. Since the stoichiometric composition of CD-MOF prepared using  $KHCO_3$  is  $K_2(C_{48}H_{80}O_{40})(HCO_3)_2$ , it is reasonable that the BET area reached the maximum at  $K^+/CD = 2$ . CD-MOF prepared at  $K^+/CD = 2$  by wash-free mechanochemical synthesis has a high BET area ( $906 m^2 g^{-1}$ ) comparable to that prepared by the conventional vapour diffusion method ( $803 m^2 g^{-1}$ ). To verify the necessity of the washing step, the nitrogen adsorption/desorption isotherm of the washed sample is shown in Fig. S5 (ESI).<sup>†</sup> The product washed after mechanochemical treatment had a reduced BET area ( $368 m^2 g^{-1}$ ). This supports that the high crystallinity of the CD-MOF is obtained by wash-free mechanochemical synthesis. This is highly correlated with the



Scheme 1 Schematic illustration of the barrel-like structure of CD linked by  $K^+$ . Note that  $K^+$  at the widest bilge of the barrel is shared with the head of the adjacent barrel.

high diffraction intensity result of the XRD pattern, as shown in Fig. 1. On the other hand, as the  $K^+/CD$  ratio decreased, the diffraction intensities attributed to the crystal structure of CD-MOF became smaller, and the BET area of CD-MOF decreased accordingly. In particular, the BET area of CD-MOF prepared with  $K^+/CD = 0.67$  is low ( $143 m^2 g^{-1}$ ), suggesting low crystallinity. It is estimated that the reduced BET area corresponds to the amorphous fraction. It has already been reported that even if the structure of CD-MOF is amorphous, it has potential applications as a drug carrier.<sup>21,22</sup> The lack of potassium (especially under conditions of  $K^+/CD < 1$ ) causes defects in the CD bonds, resulting in reduced crystallinity, as shown in Scheme 1.

There is a significant difference in the size of the crystals compared to the conventional method. While the vapor diffusion method usually yields crystals of several hundred micrometers, the particle sizes obtained by wash-free mechanochemical synthesis are from submicrons to a few micrometers, as shown in Fig. S6 (ESI).<sup>†</sup> It has been reported that the particle sizes of submicrons to a few micrometers are suitable for drug delivery systems, especially for transpulmonary formulations.<sup>21,33</sup>

This study demonstrates that CD-MOFs with high BET area can be synthesized using any type of potassium source by mechanochemical synthesis without the need for a washing step. Although the synthesis of CD-MOFs using KCl or  $CH_3COOK$  instead of KOH has been reported, in all cases reported so far, the synthesis takes a long time and/or requires additives to obtain the product.<sup>34–38</sup> Conventional synthesis methods invariably require a process to wash the products. In contrast, in our method, CD-MOFs can be synthesized in just over an hour. Furthermore, as the third component is a very small amount of ethanol, it can be easily removed by drying the product at a relatively low temperature. As shown in Fig. S7 (ESI),<sup>†</sup> drying of the product at 60 °C for 1 h is sufficient for activation.

CD-MOFs can be successfully synthesized even when the ethanol/CD ratio is reduced to 0.023 (the standard ethanol/CD ratio is 0.04). However, at lower ratios, the potassium source remains unreacted, as shown in Fig. S8 (ESI).<sup>†</sup> The role of the third component, ethanol, is therefore to facilitate mass transfer and mixing between  $\gamma$ -CD and the potassium source.<sup>24,25</sup> Under conditions with ethanol/CD ratio above 0.023, CD-MOFs can be synthesized even when the mechanochemical reaction time is reduced to 5 min, as shown in Fig. S9 (ESI).<sup>†</sup> This method can achieve both structure formation and drug delivery of CD-MOFs simultaneously. Furthermore, our method can



achieve both structure formation of CD-MOF and drug inclusion in its pores simultaneously by adding a drug as the fourth component. In this study, an antitubercular drug levofloxacin hydrate was used as a model. Levofloxacin has hydrophilic nature and can be encapsulated in the hydrophilic pores of CD-MOF. As a demonstration, levofloxacin could be successfully encapsulated in CD-MOF at 15.5 wt%, as shown in Fig. S10 (ESI).<sup>†</sup> Since the solubility of levofloxacin in ethanol is 9 mg mL<sup>-1</sup> at 25 °C, levofloxacin just adhering to the surface of CD-MOF particles can be easily washed off with ethanol. In contrast, CD-MOF is insoluble in ethanol and its structure is stable against ethanol. Levofloxacin was not eluted from the levofloxacin-encapsulated CD-MOF with ethanol, strongly indicating that levofloxacin is confined within the pores of the CD-MOF. This inclusion amount is approximately double the amount previously encapsulated by our group using the spray-drying method. One of the reasons for this difference is that CD-MOF prepared by wash-free mechanochemical synthesis has a much larger BET area than that prepared by the spray-drying method (~94.1 m<sup>2</sup> g<sup>-1</sup>).<sup>21,22</sup>

Furthermore, in this study, an antifungal drug clotrimazole was successfully encapsulated in CD-MOF at 14.6 wt% as an insoluble model drug. Due to solubility issues, it is difficult to simultaneously encapsulate both soluble and insoluble drugs in CD-MOF using liquid phase methods, including spray-drying. On the other hand, wash-free mechanochemical synthesis, which only involves milling solid mixtures, can synthesize MOF-DDS without dissolving drugs in solvent, thus enabling simultaneous encapsulation of both soluble and insoluble drugs in CD-MOF. However, when levofloxacin and clotrimazole were added simultaneously, their content in the CD-MOF carrier (levofloxacin; 11.1 wt%, clotrimazole; 13.4 wt%) was lower than those prepared by adding each drug alone.

It is important to understand the potential cytotoxicity of CD-MOF carriers prepared by the novel method, wash-free mechanochemical synthesis. Although several groups have reported on the cytotoxicity of CD-MOFs, most of these studies have been

conducted using Caco-2, the small intestine cells. Few studies have examined the toxicity of MRC-5, lung cells, or A549, alveolar cells. In commonly reported cases, cytotoxicity assessments have been carried out at concentrations up to 1 mg L<sup>-1</sup>,<sup>33,39,40</sup> whereas in this study, cytotoxicity assessments were carried out up to ultrahigh concentrations of up to 10 g L<sup>-1</sup>, as shown in Fig. 4. Incidentally, CD-MOFs prepared using KOH, KHCO<sub>3</sub>, CH<sub>3</sub>COOK and KCl showed pH 11.64, 11.24, 7.22 and 6.77 at 10 g L<sup>-1</sup> concentration in aqueous solution, respectively. Even when the concentration of CD-MOF carriers reached 10 g L<sup>-1</sup>, the viability of all three cells remained above 90%, indicating superior biocompatibility. The low cytotoxicity of CD-MOF carriers could be attributed to the non-toxic and biodegradable nature of  $\gamma$ -CD and potassium sources used. CD-MOFs prepared by wash-free mechanochemical synthesis are therefore safe for oral and transpulmonary administration.

## Conclusions

We have developed a facile strategy for the preparation of highly crystalline and high surface area CD-MOFs as drug carriers. The mechanochemical synthesis of MOFs, which requires no washing steps at all, opens the door to the mass production of MOFs and their practical applications in biochemical, pharmaceutical and food engineering. It was demonstrated that the CD-MOF carriers are safe for oral and transpulmonary administration due to their low cytotoxicity to lung, alveolar and small intestinal cells. This method also allows for simultaneous structure formation of the carrier and drug encapsulation within the pore structure by simply adding the drug during the synthesis of CD-MOFs, thus obtaining high drug content. This paper is expected to provide new concepts for the future development of advanced MOFs. On the other hand, it is unclear how the presence of potassium salts in the CD-MOF structure affects the functionality of drugs encapsulated in the carrier. Further *in vitro* and *in vivo* studies are needed to clarify the therapeutic effect of MOF-DDS.

## Conflicts of interest

There are no conflicts to declare.

## Acknowledgements

This study was supported by the Collaborative Research Center of Engineering, Medicine and Pharmacology (CEMP), Kansai University. S. T. gratefully acknowledges the support from the Iketani Science and Technology Foundation.

## Notes and references

- 1 S. Yuan, L. Feng, K. C. Wang, J. D. Pang, M. Bosch, C. Lollar, Y. J. Sun, J. S. Qin, X. Y. Yang, P. Zhang, Q. Wang, L. F. Zou, Y. M. Zhang, L. L. Zhang, Y. Fang, J. L. Li and H. C. Zhou, *Adv. Mater.*, 2018, **30**, 1704303.
- 2 A. Kirchon, L. Feng, H. F. Drake, E. A. Joseph and H. C. Zhou, *Chem. Soc. Rev.*, 2018, **47**, 8611–8638.

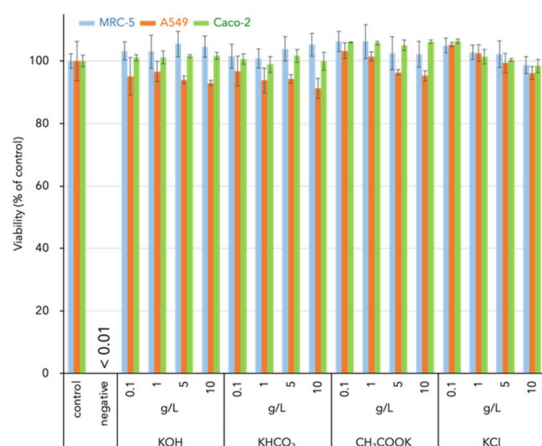


Fig. 4 *In vitro* cell viability of MRC-5, A549 and Caco-2 cells against CD-MOF carriers with different concentrations. CD-MOF prepared at K<sup>+</sup>/CD = 2 by wash-free mechanochemical synthesis. The negative reference is 1 g L<sup>-1</sup> sodium dodecyl sulfate.



- 3 S. V. Dummert, H. Saini, M. Z. Hussain, K. Yadava, K. Jayaramulu, A. Casini and R. A. Fischer, *Chem. Soc. Rev.*, 2022, **51**, 5175–5213.
- 4 R. Challa, A. Ahuja, J. Ali and R. K. Khar, *AAPS PharmSciTech*, 2005, **6**, E329–E357.
- 5 Y. Chen and Y. Liu, *Chem. Soc. Rev.*, 2010, **39**, 495–505.
- 6 G. Crini, *Chem. Rev.*, 2014, **114**, 10940–10975.
- 7 R. A. Smaldone, R. S. Forgan, H. Furukawa, J. J. Gassensmith, A. M. Z. Slawin, O. M. Yaghi and J. F. Stoddart, *Angew. Chem., Int. Ed.*, 2010, **49**, 8630–8634.
- 8 J. J. Gassensmith, H. Furukawa, R. A. Smaldone, R. S. Forgan, Y. Y. Botros, O. M. Yaghi and J. F. Stoddart, *J. Am. Chem. Soc.*, 2011, **133**, 15312–15315.
- 9 D. DeSantis, J. A. Mason, B. D. James, C. Houchins, J. R. Long and M. Veenstra, *Energy Fuels*, 2017, **31**, 2024–2032.
- 10 P. A. Julien, C. Mottillo and T. Friščić, *Green Chem.*, 2017, **19**, 2729–2747.
- 11 Z. Ni and R. I. Masel, *J. Am. Chem. Soc.*, 2006, **128**, 12394–12395.
- 12 S. H. Jhung, J. H. Lee, J. W. Yoon, C. Serre, G. Férey and J. S. Chang, *Adv. Mater.*, 2007, **19**, 121–124.
- 13 W. J. Son, J. Kim, J. Kim and W. S. Ahn, *Chem. Commun.*, 2008, **47**, 6336–6338.
- 14 D. W. Jung, D. A. Yang, J. Kim, J. Kim and W. S. Ahn, *Dalton Trans.*, 2010, **39**, 2883–2887.
- 15 M. Faustini, J. Kim, G. Y. Jeong, J. Y. Kim, H. R. Moon, W. S. Ahn and D. P. Kim, *J. Am. Chem. Soc.*, 2013, **135**, 14619–14626.
- 16 A. Polyzoidis, T. Altenburg, M. Schwarzer, S. Loebbecke and S. Kaskel, *Chem. Eng. J.*, 2016, **283**, 971–977.
- 17 K. Kida, M. Okita, K. Fujita, S. Tanaka and Y. Miyake, *CrystEngComm*, 2013, **15**, 1794–1801.
- 18 M. Yamaguchi and S. Tanaka, *J. Colloid Interface Sci.*, 2023, **638**, 513–523.
- 19 A. Carné-Sánchez, I. Imaz, M. Cano-Sarabia and D. Maspoch, *Nat. Chem.*, 2013, **5**, 203–211.
- 20 S. Tanaka and R. Miyashita, *ACS Omega*, 2017, **2**, 6437–6445.
- 21 J. Y. Tse, K. Kadota, T. Nakajima, H. Uchiyama, S. Tanaka and Y. Tozuka, *Cryst. Growth Des.*, 2022, **22**, 1143–1154.
- 22 K. Kadota, J. Y. Tse, S. Fujita, N. Suzuki, H. Uchiyama, Y. Tozuka and S. Tanaka, *ACS Appl. Bio Mater.*, 2023, **6**, 3451–3462.
- 23 A. Pichon, A. Lazuen-Garay and S. L. James, *CrystEngComm*, 2006, **8**, 211–214.
- 24 T. Friščić and L. Fabian, *CrystEngComm*, 2009, **11**, 743–745.
- 25 M. J. Cliffe, C. Mottillo, R. S. Stein, D. K. Bučarb and T. Friščić, *Chem. Sci.*, 2012, **3**, 2495–2500.
- 26 S. Tanaka, K. Kida, T. Nagaoka, T. Ota and Y. Miyake, *Chem. Commun.*, 2013, **49**, 7884–7886.
- 27 S. Tanaka, *Metal-Organic Frameworks for Biomedical Applications*, Elsevier, 2020, pp. 197–222.
- 28 Y. H. Wei, S. B. Han, D. A. Walker, P. E. Fuller and B. A. Grzybowski, *Angew. Chem., Int. Ed.*, 2012, **51**, 7435–7439.
- 29 R. S. Forgan, R. A. Smaldone, J. J. Gassensmith, H. Furukawa, D. B. Cordes, Q. W. Li, C. E. Wilmer, Y. Y. Botros, R. Q. Snurr, A. M. Z. Slawin and J. F. Stoddart, *J. Am. Chem. Soc.*, 2012, **134**, 406–417.
- 30 S. L. James, C. J. Adams, C. Bolm, D. Braga, P. Collier, T. Friščić, F. Grepioni, K. D. M. Harris, G. Hyett, W. Jones, A. Krebs, J. Mack, L. Maini, A. G. Orpen, I. P. Parkin, W. C. Shearouse, J. W. Steed and D. C. Waddell, *Chem. Soc. Rev.*, 2012, **41**, 413–447.
- 31 J. L. Do and T. Friščić, *ACS Cent. Sci.*, 2017, **3**, 13–19.
- 32 H. J. Kang, Y. H. Choi, I. W. Joo and J. E. Lee, *Bull. Korean Chem. Soc.*, 2021, **42**, 737–739.
- 33 X. X. Hu, C. F. Wang, L. B. Wang, Z. X. Liu, L. Wu, G. Q. Zhang, L. Yu, X. H. Ren, P. York, L. X. Sun, J. W. Zhang and H. Y. Li, *Int. J. Pharm.*, 2019, **564**, 153–161.
- 34 Y. Furukawa, T. Ishiwata, K. Sugikawa, K. Kokado and K. Sada, *Angew. Chem., Int. Ed.*, 2012, **51**, 10566–10569.
- 35 S. S. Wang, X. Yang, W. X. Lu, N. Y. Jiang, G. Q. Zhang, Z. E. Cheng and W. J. Liu, *J. Drug Delivery Sci. Technol.*, 2021, **64**, 102593.
- 36 M. E. Zick, S. M. Pugh, J. H. Lee, A. C. Forse and P. J. Milner, *Angew. Chem., Int. Ed.*, 2022, **61**, e202206718.
- 37 J. Rodriguez-Martinez, M. J. Sánchez-Martín, O. López-Patarroyo and M. Valiente, *J. Drug Delivery Sci. Technol.*, 2022, **79**, 104085.
- 38 X. D. Pan, S. A. Junejo, C. P. Tan, B. Zhang, X. Fu and Q. Huang, *J. Sci. Food Agric.*, 2022, **102**, 6387–6396.
- 39 C. Qiu, D. J. McClements, Z. Y. Jin, C. X. Wang, Y. Qin, X. M. Xu and J. P. Wang, *J. Colloid Interface Sci.*, 2019, **553**, 549–556.
- 40 N. Ji, Y. Hong, Z. B. Gu, L. Cheng, Z. F. Li and C. M. Li, *J. Agric. Food Chem.*, 2017, **65**, 8866–8874.

